Int. J. Multiphase Flow, Vol. 1, pp. 411–436. Pergamon Press, 1974. Printed in Great Britain.

THE EFFECT OF HYDRODYNAMIC COUPLING ON THE AXISYMMETRIC DRAINAGE OF THIN FILMS

X. B. REED, JR., E. RIOLO and S. HARTLAND
Technisch-Chemisches Laboratorium, Eidgenössische Technische Hochschule Zürich, Switzerland

(*Received* 1 *September* 1973)

Abstract—The effect of hydrodynamic coupling of adjacent phases on the axisymmetric drainage of thin films is examined using a prototype model of coalescence. For long times, pressure forces in the film dominate flow in all three regions, and finally all move effectively as one, whereas for short times, profiles are sharp and initial flow differences in the three regions can dominate pressure effects. For intermediate times, temporal evolution of velocity profiles depends in a complicated way on the kinematic viscosity ratio and the parameter $R = (\rho_A\mu_A/\rho_B/\mu_B)^{1/2}$, as well as on initial conditions and pressure gradient. Generally speaking, the initial flows have less of an effect on overall drainage time than the presence of induced circulation in adjacent phases. Analytical solutions are plotted for a range of systems and representative initial conditions and pressure gradients. In a subsequent article, film-thinning equations are solved using this information.

1. INTRODUCTION

The approach of a drop to another drop or a deformable bulk interface is determined by the rate of drainage of the intervening fluid film (Hartland 1970). When the film becomes thin enough, it ruptures, culminating the final stage of the overall coalescence process. For the gravitational approach of two drops of different size or a drop to a bulk interface, the overall shape of the draining film is spherical (Princen 1963). For two equisized drops, however, the film is planar (Scheele & Leng 1971), and in any event is often axisymmetric and approximately uniform in thickness (Robinson & Hartland 1971). Moreover, for the case of equisized drops approaching vertically, there is no hydrostatic pressure gradient within the film. These are the basic ingredients of the model analyzed in Section 2.

In earlier studies of drainage of thin films, the dimensions and physical properties of the film and its bounding interfaces (Robinson & Hartland 1972; Hartland 1972) were usually included, as well as the radial component of the dynamic pressure gradient within the film; the last may result from other than gravitational forces pressing upon the film (Wood & Hartland 1972; Hartland & Wood 1973). If the interfaces are not immobilized by surface active agent(s), however, the fluid motion in the contiguous phases will be coupled with the motion within the film—and therefore ultimately with one another, as well. As a consequence of hydrodynamic coupling, then, the drainage of the film must also depend upon the physical properties and the circulation patterns within the drop and its homophase. Previous models have considered the film to be uniform in thickness and either fully mobile ("free", in conventional hydrodynamic usage) or completely immobile (Reynolds 1886; Hartland 1967; Riolo, Reed & Hartland 1973); the former approximate to gas–liquid interfaces, the latter to solid surfaces, liquid interfaces saturated with surface active agent, or extremely viscous contiguous phases.

The models have also been refined to allow for small deformations of immobile or free interfaces due to the pressure gradient within the film, the pressure difference across the interface being balanced by the normal component of the surface stress arising from local curvature and interfacial tension (Hartland 1969). No model has as yet considered the effect of motion within the adjacent phases, however, although there is ample experimental evidence of the effect in clean systems (Hartland 1969). An attempt has been made (Murdoch & Leng 1971) to explain experiments on colliding drops (Scheel & Leng 1971) in terms of a model in which circulation within the drops was felt to be important; similar experiments had already been carried out on colliding drops (Allan & Mason 1962; McKay & Mason 1964). Certainly drop circulation will set in during the unconstrained approach of a clean drop to an interface which will both enhance, and be enhanced by, the outward drainage of the intervening film, but this can be countered by inertial effects resulting from impact and subsequent deformation and flattening of the drop, with the result that circulation can even be reversed, thereby dragging liquid back into the film and leading to dimpling (Hartland 1970, 1969). Despite the considerable effect of these inertial forces and resultant initial circulation patterns within adjacent phases, however, the pressure gradient eventually restores normal, that is outward, drainage with associated outward circulation within adjacent phases. The role of such hydrodynamic coupling of film motion and circulation in adjacent phases is considered in this paper, with the concomitant effect on film-thinning taken up in a subsequent one.

2. FORMULATION AND SOLUTION OF THE HYDRODYNAMIC EQUATIONS

The basic simplifying assumptions in the earlier drainage models, aside from the boundary conditions, are those familiar in the hydrodynamic theory of lubrication, namely the quasi-static assumption and the essential one-dimensionality of flow. These ingredients are retained in this model, the former in somewhat generalized form. The pressure field varies radially but not vertically, thereby only driving the fluid radially, the orthogonal direction having negligible motion. The location of the interfaces changes only slowly, so that the "instantaneous" solutions of the hydrodynamic equations are obtained as though the interfaces were stationary, the form which the quasi-static assumption takes for this problem.

At an uncontaminated liquid–liquid interface, the basic conditions to be satisfied are a balance of pressure forces by surface tension, a balance of viscous stresses, and continuity of velocity.

The drainage of the film often proceeds with an essentially constant thickness, making the surface tension boundary condition redundant in so far as the hydrodynamics are concerned; conversely, when appreciable deformation of the interface takes place which would bring surface tension into play, the basic drainage assumptions soon thereafter become invalid. Consequently, that boundary condition is considered no further.

The weight, or buoyancy, of the drop acting in distributed form over the interface delineating the film squeezes the fluid out of the film, and the film flow may or may not begin from a state of rest. The motion in the film is thus generally time-dependent, and this is true even for the simpler models for which the velocity fields are implicitly dependent upon the time (see Riolo, Reed & Hartland (1973) for an analysis of explicit transients within the context of Reynolds' model). For real systems, the motion in the film acts through the *velocity and momentum flux continuity conditions* to set the liquid in the drop and its homophase in motion. The motion in those two regions is thus *explicitly* time-dependent, as is necessarily also that in the draining film. It is the *time-dependent coupling of the motion in the three regions which makes the hydrodynamic problem nontrivial despite its linearity.*

Under the stated conditions the equations describing the fluid motion are (see figure 1 for a schematic):

$$\left(\frac{\partial^2}{\partial z^2} - \frac{1}{\nu_A}\frac{\partial}{\partial t}\right) v_r^A = -\frac{k}{\nu_A} \equiv +\frac{1}{\nu_A}\frac{\partial}{\partial r}(p_A/\rho_A) = \frac{1}{\mu_A}\frac{\partial p_A}{\partial r}, \qquad [1]$$

$$\left(\frac{\partial^2}{\partial z^2} - \frac{1}{\nu_B}\frac{\partial}{\partial t}\right) v_r^B = 0, \qquad B = B_1, B_2 \qquad [2, 3]$$

where v and μ are the kinematic and dynamic viscosities and ρ is the density; $k = -(1/\rho_A)(\partial p/\partial r)$ is the effective/pressure gradient; p is the local pressure; v_r is the radial velocity; z is the vertical distance and r is the radial distance in film.

Subject to the following boundary conditions:

$$\text{at} \quad z = 0: \; v_r^A = v_r^{B_2}, \qquad \mu_A \frac{\partial v_r^A}{\partial z} = \mu_B \frac{\partial v_r^{B_2}}{\partial z}, \qquad [4a, b]$$

$$\text{at} \quad z = \delta: \; v_r^A = v_r^{B_1}, \qquad \mu_A \frac{\partial v_r^A}{\partial z} = \mu_B \frac{\partial v_r^{B_1}}{\partial z}, \qquad [5a, b]$$

$$\text{as} \quad z \to \infty: \; v_r^{B_1} \to v_o^1, \qquad [6]$$

$$\text{as} \quad z \to -\infty: \; v_r^{B_2} \to v_o^2. \qquad [7]$$

Superscript A refers to the fluid in the film, while B_1 and B_2 denote the drop and its homophase.

Because the motion is time dependent, initial conditions must also be specified, but because of the difficulty in knowing the precise conditions at the onset of validity of the drainage equations, and because of the complexity of considering quite general initial flow fields, we suppose that at time zero the velocity fields are as follows:

$$\text{at} \quad t = 0: \; v_r^A = u_o, \quad v_r^{B_1} = v_o^1, \quad v_r^{B_2} = v_o^2, \qquad [8]$$

with the initial conditions being at most functions of r and slowly varying functions of z which should decrease at great distances from the interfaces. v_o^1 and v_o^2 are the initial radial velocities in phases B_1 and B_2.

If
$$\tilde{u}_A = \mathscr{L}\{v_r^A\}, \quad \tilde{u}_{B_1} = \mathscr{L}\{v_r^{B_1}\},$$
$$\tilde{u}_{B_2} = \mathscr{L}\{v_r^{B_2}\}, \quad \text{and} \quad \tilde{k} = \mathscr{L}\left\{-\frac{\partial}{\partial r}(p_A/\rho_A)\right\}$$

denote the Laplace transforms of the several dependent variables, then the ancillary equations are

$$\left(\frac{\mathrm{d}^2}{\mathrm{d}z^2} - q_A^2\right)\tilde{u}_A = -\frac{1}{\nu_A}(\tilde{k} + u_o), \tag{9}$$

$$\left(\frac{\mathrm{d}^2}{\mathrm{d}z^2} - q_B^2\right)\tilde{u}_{B_1} = -\frac{v_o^1}{\nu_B}, \tag{10}$$

$$\left(\frac{\mathrm{d}^2}{\mathrm{d}z^2} - q_B^2\right)\tilde{u}_{B_2} = -\frac{v_o^2}{\nu_B}. \tag{11}$$

Corresponding solutions are

$$\tilde{u}_A = c_1 e^{q_A z} + c_2 e^{-q_A z} - \left(\frac{\tilde{k} + u_o}{2\nu_A q_A^2}\right)[e^{q_A z} + e^{-q_A z} - 2], \tag{12}$$

$$\tilde{u}_{B_1} = c_3 e^{q_B z} + c_4 e^{-q_B z} - \frac{v_o^1}{\nu_B q_B^2}[e^{-q_B z} - 1], \tag{13}$$

$$\tilde{u}_{B_2} = c_5 e^{q_B z} + c_6 e^{-q_B z} - \frac{v_o^2}{\nu_B q_B^2}[e^{q_B z} - 1], \tag{14}$$

in which $q = (s/\nu)^{1/2}$ and s is the Laplace-transform variable. The constants c_1–c_6 as determined from the transformed boundary conditions after some algebra are

$$c_3 = c_6 = 0$$

$$c_1 = \frac{\tilde{k} + u_o}{2\nu_A q_A^2}\left(\frac{R+1}{D}\right)[(R+1)e^{q_A\delta} - (R-1)e^{-q_A\delta} - 2] + \frac{v_o^1}{\nu_B q_B^2}\left(\frac{R+1}{D}\right) + \frac{v_o^2}{\nu_B q_B^2}\left(\frac{R-1}{D}\right)e^{-q_A\delta}, \tag{15}$$

$$c_2 = \frac{\tilde{k} + u_o}{2\nu_A q_A^2}\left(\frac{R-1}{D}\right)[(R+1)e^{q_A\delta} - (R-1)e^{-q_A\delta} - 2] + \frac{v_o^1}{\nu_B q_B^2}\left(\frac{R-1}{D}\right) + \frac{v_o^2}{\nu_B q_B^2}\left(\frac{R+1}{D}\right)e^{q_A\delta}, \tag{16}$$

$$c_4 = \frac{\tilde{k} + u_o}{\nu_A q_A}\left(\frac{R}{D}\right)[(R+1)e^{Q_+\delta} - (R-1)e^{Q_-\delta} - 2e^{q_B\delta}]$$

$$- \frac{v_o^1}{\nu_B q_B^2}\left(\frac{R}{D}\right)[(R+1)e^{Q_+\delta} - (R-1)e^{Q_-\delta}]$$

$$+ \frac{v_o^1}{\nu_B q_B^2} + \frac{v_o^2}{\nu_B q_B^2}\left(\frac{2R}{D}\right)e^{q_B\delta}, \qquad [17]$$

$$c_5 = \frac{\tilde{k} + u_o}{\nu_A q_A^2}\left(\frac{R}{D}\right)[(R+1)e^{q_A\delta} - (R-1)e^{-q_A\delta} - 2]$$

$$+ \frac{v_o^1}{\nu_B q_B^2}\left(\frac{2R}{D}\right) + \frac{v_o^2}{\nu_B q_B^2}\left(\frac{1}{D}\right)[(R+1)e^{q_A\delta} + (R-1)e^{-q_A\delta}], \qquad [18]$$

in which δ is the film thickness and

$$D = (R+1)^2 e^{q_A\delta} - (R-1)^2 e^{-q_A\delta}. \qquad [19]$$

In these formulae, $R = \frac{\mu_A q_A}{\mu_B q_B} = \left(\frac{\mu_A}{\mu_B}\right)\left(\frac{\nu_B}{\nu_A}\right)^{1/2} = \left(\frac{\rho_A \mu_A}{\rho_B \mu_B}\right)^{1/2}$ represents the relation between momentum transport at the boundary between the two phases (as measured by the dynamic viscosity ratio) and momentum transport in the interior of the two phases (as measured by the square root of the kinematic viscosity ratio). The remaining parameters are

$$Q_+ = q_B + q_A, \qquad Q_- = q_B - q_A.$$

Consequently, the transformed velocities are given, upon assuming the pressure to vary at most slowly and after some re-arrangement, by

$$\tilde{u}_A = -\left(\frac{\tilde{k} + u_o}{\nu_A q_A^2}\right)\left(\frac{1}{D}\right)[(R+1)e^{q_A(\delta - z)} + (R-1)e^{-q_A(\delta - z)}$$

$$+ (R+1)e^{q_A z} + (R-1)e^{-q_A z}] + \left(\frac{\tilde{k} + u_o}{\nu_A q_A^2}\right) + \left(\frac{v_o^1}{\nu_B q_B^2}\right)\left(\frac{1}{D}\right)[(R+1)e^{q_A z}$$

$$+ (R-1)e^{-q_A z}] + \left(\frac{v_o^2}{\nu_B q_B^2}\right)\left(\frac{1}{D}\right)[(R+1)e^{q_A(\delta - z)} + (R-1)e^{-q_A(\delta - z)}], \qquad [20]$$

$$\tilde{u}_{B_1} = \left(\frac{\tilde{k} + u_o}{\nu_A q_A^2}\right)\left(\frac{R}{D}\right)[(R+1)e^{q_B(\delta - z) + q_A\delta} - (R-1)e^{q_B(\delta - z) - q_A\delta} - 2e^{q_B(\delta - z)}]$$

$$- \frac{v_o^1}{\nu_B q_B^2}\left(\frac{R}{D}\right)[(R+1)e^{q_B(\delta - z) + q_A\delta} - (R-1)e^{q_B(\delta - z) - q_A\delta}]$$

$$+ \frac{v_o^1}{\nu_B q_B^2} + \frac{v_o^2}{\nu_B q_B^2}\left(\frac{2R}{D}\right)e^{q_B(\delta - z)}, \qquad [21]$$

$$\tilde{u}_{B_2} = \left(\frac{\tilde{k} + u_o}{\nu_A q_A^2}\right)\left(\frac{R}{D}\right)[(R+1)e^{q_B z + q_A\delta} - (R-1)e^{q_B z - q_A\delta} - 2e^{q_B z}]$$

$$+ \frac{v_o^1}{\nu_B q_B^2}\left(\frac{2R}{D}\right)e^{q_B z} + \frac{v_o^2}{\nu_B q_B^2} - \frac{v_o^2}{\nu_B q_B^2}\left(\frac{R}{D}\right)[(R+1)e^{q_B z + q_A\delta} - (R-1)e^{q_B z - q_A\delta}]. \qquad [22]$$

These expressions only apparently lack inverses, for D contains exponentials which insure their existence. Because of their complexity, however, [20]–[22] cannot be immediately inverted, but can be manipulated into known forms using standard methods which are applied below (Carslaw & Jaeger 1959). Because of the resultant series solutions, it is worthwhile commenting on the more readily interpreted transformed solutions.

The result for the transformed film velocity provides for an equivalent influence by the flows in the other two regions and for a symmetric velocity field provided $v_o^1 = v_o^2$. The way in which initial flow in B_2 influences motion in B_1 is seen from [21] and [22] to be the same as the way in which initial flow in B_1 influences motion in B_2. The entire flow field in B_1–A–B_2 is symmetric if $v_0^1 = v_0^2$. The initial flow in the film also enters the expressions for drop and homophase in a symmetrical manner. Finally, the role of the pressure gradient in driving the film flow is seen to be propagated by hydrodynamic coupling into an *explicit* role in the flow fields in the remaining two phases.

Although not crucial to our development, the assumption that there is virtually no temporal variation of the pressure field during drainage does simplify matters considerably. More importantly, there is appreciable indirect experimental support for this contention. Although direct measurements of pressures and velocities within such thin films have not been made, the deformation of a fluid interface is an especially sensitive indicator of a change in pressure during drainage. Often interfacial deformation is small or nonexistent; and when dimpling is appreciable, it serves to relieve build-up of pressure. Also qualitative observations of velocity fields in the neighboring phases indicate general agreement with our subsequent predictions (Section 4). Perhaps the most significant support is provided by the film-thinning curves calculated on the basis of the same assumption in the following article: the theoretical predictions are not only qualitatively correct, they are quantitatively accurate.

The solutions to the ancillary equations yield, upon inversion, the velocity fields in the drop (B_1) and its homophase (B_2) and the film of continuous phase (A) remaining between them. Already a bit complicated, their inversion yields still more complicated expressions:

$$
\begin{aligned}
v_r^A = {} & -\frac{4kt}{(R+1)^2}\sum_{n=0}^{\infty}\left(\frac{R-1}{R+1}\right)^{2n}\left\{(R+1)i^2\operatorname{erfc}\left[\frac{2n\delta+z}{2(\nu_A t)^{1/2}}\right]+(R-1)i^2\operatorname{erfc}\left[\frac{(2n+2)\delta-z}{2(\nu_A t)^{1/2}}\right]\right.\\
& \left.+(R+1)i^2\operatorname{erfc}\left[\frac{(2n+1)\delta-z}{2(\nu_A t)^{1/2}}\right]+(R-1)i^2\operatorname{erfc}\left[\frac{(2n+1)\delta+z}{2(\nu_A t)^{1/2}}\right]\right\}+kt\\
& -\frac{u_o}{(R+1)^2}\sum_{n=0}^{\infty}\left(\frac{R-1}{R+1}\right)^{2n}\left\{(R+1)\operatorname{erfc}\left[\frac{2n\delta+z}{2(\nu_A t)^{1/2}}\right]+(R-1)\operatorname{erfc}\left[\frac{(2n+2)\delta-z}{2(\nu_A t)^{1/2}}\right]\right.\\
& \left.+(R+1)\operatorname{erfc}\left[\frac{(2n+1)\delta-z}{2(\nu_A t)^{1/2}}\right]+(R-1)\operatorname{erfc}\left[\frac{(2n+1)\delta+z}{2(\nu_A t)^{1/2}}\right]\right\}+u_o\\
& +\frac{v_o^1}{(R+1)^2}\sum_{n=0}^{\infty}\left(\frac{R-1}{R+1}\right)^{2n}\left\{(R+1)\operatorname{erfc}\left[\frac{(2n+1)\delta-z}{2(\nu_A t)^{1/2}}\right]+(R-1)\operatorname{erfc}\left[\frac{(2n+1)\delta+z}{2(\nu_A t)^{1/2}}\right]\right\}\\
& +\frac{v_o^2}{(R+1)^2}\sum_{n=0}^{\infty}\left(\frac{R-1}{R+1}\right)^{2n}\left\{(R+1)\operatorname{erfc}\left[\frac{2n\delta+z}{2(\nu_A t)^{1/2}}\right]+(R-1)\operatorname{erfc}\left[\frac{(2n+2)\delta-z}{2(\nu_A t)^{1/2}}\right]\right\}. \qquad [23]
\end{aligned}
$$

$$
\begin{aligned}
v_r^{B_1} = {} & 4kt \frac{R}{(R+1)^2} \sum_{n=0}^{\infty} \left(\frac{R-1}{R+1}\right)^{2n} \times \left\{ (R+1) i^2\mathrm{erfc}\left[\frac{(z-\delta)+(\nu_B/\nu_A)^{1/2}2n\delta}{2(\nu_B t)^{1/2}}\right] \right. \\
& \left. -(R-1) i^2\mathrm{erfc}\left[\frac{(z-\delta)+(\nu_B/\nu_A)^{1/2}(2n+2)\delta}{2(\nu_B t)^{1/2}}\right] - 2i^2\mathrm{erfc}\left[\frac{(z-\delta)+(\nu_B/\nu_A)^{1/2}(2n+1)\delta}{2(\nu_B t)^{1/2}}\right]\right\} \\
& + u_o \frac{R}{(R+1)^2} \sum_{n=0}^{\infty} \left(\frac{R-1}{R+1}\right)^{2n} \left\{ (R+1)\mathrm{erfc}\left[\frac{(z-\delta)+(\nu_B/\nu_A)^{1/2}2n\delta}{2(\nu_B t)^{1/2}}\right] \right. \\
& \left. -(R-1)\mathrm{erfc}\left[\frac{(z-\delta)+(\nu_B/\nu_A)^{1/2}(2n+2)\delta}{2(\nu_B t)^{1/2}}\right] - 2\,\mathrm{erfc}\left[\frac{(z-\delta)+(\nu_B/\nu_A)^{1/2}(2n+1)\delta}{2(\nu_B t)^{1/2}}\right]\right\} \\
& - v_o^1 \frac{R}{(R+1)^2} \sum_{n=0}^{\infty} \left(\frac{R-1}{R+1}\right)^{2n} \left\{ (R+1)\mathrm{erfc}\left[\frac{(z-\delta)+(\nu_B/\nu_A)^{1/2}2n\delta}{2(\nu_B t)^{1/2}}\right] \right. \\
& \left. -(R-1)\mathrm{erfc}\left[\frac{(z-\delta)+(\nu_B/\nu_A)^{1/2}(2n+2)\delta}{2(\nu_B t)^{1/2}}\right]\right\} + v_o^1 \\
& + v_o^2 \frac{2R}{(R+1)^2} \sum_{n=0}^{\infty} \left(\frac{R-1}{R+1}\right)^{2n} \mathrm{erfc}\left[\frac{(z-\delta)+(\nu_B/\nu_A)^{1/2}(2n+1)\delta}{2(\nu_B t)^{1/2}}\right],
\end{aligned} \quad [24]
$$

$$
\begin{aligned}
v_r^{B_2} = {} & 4kt \frac{R}{(R+1)^2} \sum_{n=0}^{\infty} \left(\frac{R-1}{R+1}\right)^{2n} \left\{ (R+1) i^2\mathrm{erfc}\left[\frac{-z+(\nu_B/\nu_A)^{1/2}2n\delta}{2(\nu_B t)^{1/2}}\right] \right. \\
& \left. -(R-1) i^2\mathrm{erfc}\left[\frac{-z+(\nu_B/\nu_A)^{1/2}(2n+2)\delta}{2(\nu_B t)^{1/2}}\right] - 2i^2\mathrm{erfc}\left[\frac{-z+(\nu_B/\nu_A)^{1/2}(2n+1)\delta}{2(\nu_B t)^{1/2}}\right]\right\} \\
& + u_o \frac{R}{(R+1)^2} \sum_{n=0}^{\infty} \left(\frac{R-1}{R+1}\right)^{2n} \left\{ (R+1)\mathrm{erfc}\left[\frac{-z+(\nu_B/\nu_A)^{1/2}2n\delta}{2(\nu_B t)^{1/2}}\right] \right. \\
& \left. -(R-1)\mathrm{erfc}\left[\frac{-z+(\nu_B/\nu_A)^{1/2}(2n+2)\delta}{2(\nu_B t)^{1/2}}\right] - 2\,\mathrm{erfc}\left[\frac{-z+(\nu_B/\nu_A)^{1/2}(2n+1)\delta}{2(\nu_B t)^{1/2}}\right]\right\} \\
& + v_o^1 \frac{2R}{(R+1)^2} \sum_{n=0}^{\infty} \left(\frac{R-1}{R+1}\right)^{2n} \mathrm{erfc}\left[\frac{-z+(\nu_B/\nu_A)^{1/2}(2n+1)\delta}{2(\nu_B t)^{1/2}}\right] \\
& - v_o^2 \frac{R}{(R+1)^2} \sum_{n=0}^{\infty} \left(\frac{R-1}{R+1}\right)^{2n} \left\{ (R+1)\mathrm{erfc}\left[\frac{-z+(\nu_B/\nu_A)^{1/2}2n\delta}{2(\nu_B t)^{1/2}}\right] \right. \\
& \left. -(R-1)\mathrm{erfc}\left[\frac{-z+(\nu_B/\nu_A)^{1/2}(2n+2)\delta}{2(\nu_B t)^{1/2}}\right]\right\} + v_o^2 .
\end{aligned} \quad [25].
$$

The binomial expansion of the denominator D permitted the solutions to be obtained in the form of complementary error functions (erfc) and their repeated integrals (i^2erfc), which are tabulated functions (Abramowitz & Stegun 1968) arising in similar heat transfer problems (Carslaw & Jaeger 1959). This form for the solution also permits physical interpretation. The term kt represents a local momentum source in the film which can vary radially since $k = k(r)$. The first series can be interpreted crudely as a superposition of individual modes of momentum transfer from the film due to instantaneous values of momentum sources within the film. The constant term u_o denotes the "ground-state" of the film, from which departures are measured as indicated by the remaining terms in the solution. The other u_o-term, the second series in the solution, corresponds to diffusive interaction of the film with its two contiguous phases, with the first pair of terms representing interaction with phase B_1, the second pair interaction with phase B_2. This becomes more transparent if the u_o, v_o^1 and v_o^2 terms are grouped as

$$-\frac{(u_o - v_o^1)}{(R+1)^2}\sum_{n=0}^{\infty}\left(\frac{R-1}{R+1}\right)^{2n}\left\{(R+1)\operatorname{erfc}\left[\frac{(2n+1)\delta - z}{2(\nu_A t)^{1/2}}\right] + (R-1)\operatorname{erfc}\left[\frac{(2n+1)\delta + z}{2(\nu_A t)^{1/2}}\right]\right\}$$
$$-\frac{(u_o - v_o^2)}{(R+1)^2}\sum_{n=0}^{\infty}\left(\frac{R-1}{R+1}\right)^{2n}\left\{(R+1)\operatorname{erfc}\left[\frac{2n\delta + z}{2(\nu_A t)^{1/2}}\right] + (R-1)\operatorname{erfc}\left[\frac{(2n+2)\delta - z}{2(\nu_A t)^{1/2}}\right]\right\}.$$

The first terms (series) in $v_r^{B_1}$ and $v_r^{B_2}$ reflect the fact that the pressure gradient drives the motion within the film; the film motion, in turn, drives the motion within the contiguous phases. The remaining terms in both correspond to momentum diffusion into or out of the drop from the film and across the film into or out of its homophase, and conversely. By rearranging, for instance, the non-pressure terms in $v_r^{B_1}$ we get:

$$(u_o - v_o^1)\frac{R}{(R+1)^2}\sum_{n=0}^{\infty}\left(\frac{R-1}{R+1}\right)^{2n}\left\{(R+1)\operatorname{erfc}\left[\frac{(z-\delta) + (\nu_B/\nu_A)^{1/2}2n\delta}{2(\nu_B t)^{1/2}}\right]\right.$$
$$\left. - (R-1)\operatorname{erfc}\left[\frac{(z-\delta) + (\nu_B/\nu_A)^{1/2}(2n+2)\delta}{2(\nu_B t)^{1/2}}\right]\right\}$$
$$+ (v_o^2 - u_o)\frac{2R}{(R+1)^2}\sum_{n=0}^{\infty}\left(\frac{R-1}{R+1}\right)^{2n}\operatorname{erfc}\left[\frac{(z-\delta) + (\nu_B/\nu_A)^{1/2}(2n+1)\delta}{2(\nu_B t)^{1/2}}\right],$$

yielding directly the desired interpretation, first, of momentum diffused into the drop from the film and second, of momentum diffused through the film from the homophase.

The same complexity that makes interpretation difficult makes it desirable to consider limiting forms of the three solutions. These asymptotic forms serve as touchstones when considering the full solutions, but in some cases they are more readily obtained through the subsidiary solutions.

The equations and solutions may be made dimensionless in a natural manner, and although the figures are labelled with dimensionless coordinates, [23]–[25] will not be rewritten.

3. SOME ASYMPTOTIC FORMS OF THE ANALYTICAL SOLUTION

For large positive values of $(z - \delta)$ and large negative values of z, one recovers the undisturbed initial drop and homophase motions, respectively, because the transient fields developing in the neighborhood of the film cannot penetrate that deeply into the interior in a finite time. Thus,

$$\lim_{(z-\delta)\to\infty} v_r^{B_1} = v_o^1,$$

$$\lim_{(z\to-\infty)} v_r^{B_2} = v_o^2,$$

as is clear from [21] and [22].

Pronounced dimpling of a film may imply that flow within the film is or has been radially inward, and because of hydrodynamic coupling this should also be true in the contiguous phases. Although the solutions to the drainage equations do not remain valid for pronounced dimpling, its onset can be sought in the exact solutions. An estimate of the effect can be obtained from the drop and homophase motions in the thin-film approximation, in which case one obtains, for instance,

$$\lim_{\delta\to 0} v_r^{B_1} = k\left(\frac{R}{\nu_A^{1/2}}\right)\left(\frac{\delta}{2}\right)(4t)^{1/2} i^1\,\mathrm{erfc}\left(\frac{\delta - z}{2(\nu_B t)^{1/2}}\right)$$

$$+ u_o\left(\frac{R}{\nu_A^{1/2}}\right)\left(\frac{\delta}{2}\right)\frac{\exp\left(\frac{(z-\delta)^2}{4\nu_B t}\right)}{(\pi t)^{1/2}} - \frac{v_o^1 - v_o^2}{2}\,\mathrm{erfc}\left(\frac{z-\delta}{2(\nu_B t)^{1/2}}\right)$$

$$-\frac{1}{2}\left[\frac{(R^2-1)}{R^2}v_o^1 + \frac{(R^2+1)}{R^2}v_o^2\right]\left(\frac{R}{\nu_A^{1/2}}\right)\left(\frac{\delta}{2}\right)\frac{\exp\left(\frac{(z-\delta)^2}{4\nu_B t}\right)}{(\pi t)^{1/2}} + v_o^1. \qquad [26]$$

The several terms in the asymptotic solution for a very thin film can be viewed as contributions of individual physical effects which are superposed to give the total flow.

The first terms, quantifying the role of the pressure gradient in the film on the flow in the drop in the thin-film approximation, corresponds to a constant flux of momentum into the drop from the film. The second term can be regarded as the contribution of momentum released by the film at the initial instant and proportional to the initial flow within the film. Depending upon whether $v_o^1 \gtrless v_o^2$, the third term represents the diffusive contribution to drop flow from an initially faster homophase motion or reduction in drop momentum because momentum diffuses from it through the film and into an initially slower homophase. The fourth term is easier to interpret in view of the interpretation of the second and by grouping certain terms as below, [27]: if motion in the film is initially greater than a property weighted average of the drop and homophase motions, a proportional amount of momentum released at the film at time zero would subsequently diffuse into the drop at the rate prescribed by the rewritten fourth terms and conversely, according to

$$\lim_{\delta\to 0} v_r^{B_1} = kR\left(\frac{\delta}{2}\right)\left(\frac{4t}{\nu_A}\right)^{1/2} i^1\,\mathrm{erfc}\left(\frac{z-\delta}{2(\nu_B t)^{1/2}}\right) - \frac{(v_o^1 - v_o^2)}{2}\,\mathrm{erfc}\left(\frac{z-\delta}{2(\nu_B t)^{1/2}}\right) + v_o^1$$

$$+\left\{u_o-\frac{1}{2}\left[\left(\frac{R^2-1}{R^2}\right)v_o^1+\left(\frac{R^2+1}{R^2}\right)v_o^2\right]\right\}R\left(\frac{\delta}{2}\right)\frac{\exp\left(\frac{-(z-\delta)^2}{4\nu_B t}\right)}{(\pi\nu_A t)^{1/2}}. \quad [27]$$

The third term is simply a quantification of the "ground-state" of motion within the film, the remaining terms representing departures from that initial motion and resultant momentum diffusion.

The corresponding terms for the homophase motion in the thin-film approximation represent individual effects which are interpreted in precisely the same manner, the superposition of which gives the total homophase motion as measured from its initial motion due to pressure-driven flow in the film, due to interaction across the film (momentum exchange), and due to interaction with the film itself (via the property-weighted average), respectively:

$$\lim_{\delta\to 0} v_r^{B_2} = kR\left(\frac{\delta}{2}\right)\left(\frac{4t}{\nu_A}\right)^{1/2} i^1\operatorname{erfc}\left(\frac{-z}{(4\nu_B t)^{1/2}}\right)+\frac{(v_o^1-v_o^2)}{2}\operatorname{erfc}\left(\frac{-z}{2(\nu_B t)^{1/2}}\right)+v_o^2$$

$$+\left\{u_o-\frac{1}{2}\left[\left(\frac{R^2+1}{R^2}\right)v_o^1+\left(\frac{R^2-1}{R^2}\right)v_o^2\right]\right\}R\left(\frac{\delta}{2}\right)\frac{\exp\left(\frac{-z^2}{4\nu_B t}\right)}{(\pi\nu_A t)^{1/2}}. \quad [28]$$

The roles of v_o^1 and v_o^2, naturally, are interchanged in $v_r^{B_1}$ and $v_r^{B_2}$.

It is intuitively expected that initial conditions will be more dominant, the shorter the time. If the asymptotic forms

$$i^2\operatorname{erfc} x \sim \frac{e^{-x^2}}{4(\pi)^{1/2}x^3}$$

and

$$\operatorname{erfc} x \sim \frac{e^{-x^2}}{(\pi)^{1/2}x}$$

are introduced into the exact solution, then a term-by-term comparison of the k and the $(u_o - v_o^1)$, respectively $(u_o - v_o^2)$, terms can be made. The first term is typical, in which case the comparison comes down to the pressure-term differing by the dimensionless factor (T/ζ^2) from the $(u_o - v_o^2)$ term. For sufficiently short times, then, the pressure effect will be less than the effect of the initial conditions.

Moreover, a similar analysis of the velocity expressions in B_1 and B_2 shows that for short times the effect of the initial conditions in the adjacent phases differs by the factor R from corresponding terms in the film. Consequently, for large R the initial departure from the initial velocity in the film is magnified by the factor R in the neighboring phase and conversely. These calculations also show that the smaller the pressure gradient, the more prominent the effect is.

Of perhaps more significance than the above spatially asymptotic solutions and the temporally asymptotic solution for short times is the long-time solution, for the time at which the drainage equations become valid approximations and the conditions prevailing at that time are presently ill defined. Unfortunately, the long-time asymptote must be interpreted with reservations, as well, for the longer drainage proceeds the more likely it becomes that one or another of the assumptions underlying the drainage equations comes into question. Nevertheless, the lengthy drainage times relative to all other time scales in the overall coalescence process—an effect the more pronounced in viscous systems—invite consideration of the long-time asymptotes, which are given by:

$$\lim_{t\to\infty} v_r^A = k\frac{R}{(\pi\nu_A)^{1/2}}\,\delta t^{1/2} + \frac{v_o^1 + v_o^2}{2} + u_o\frac{R}{(\pi\nu_A)^{1/2}}\frac{\delta}{2}t^{-1/2} - \frac{1}{(\pi\nu_A)^{1/2}R}\left[(R^2+1)\frac{\delta}{2}\left(\frac{v_o^1+v_o^2}{2}\right) - \left(\frac{zv_o^1 - (z-\delta)v_o^2}{2}\right)\right]t^{-1/2}, \qquad [29]$$

$$\lim_{t\to\infty} v_r^{B_1} = k\frac{R}{(\pi\nu_A)^{1/2}}\,\delta t^{1/2} + \frac{v_o^1 + v_o^2}{2} + u_o\frac{R}{(\pi\nu_A)^{1/2}}\frac{\delta}{2}t^{-1/2} - \frac{1}{(\pi\nu_B)^{1/2}}\left[\frac{(R^2-1)v_o^1 + (R^2+1)v_o^2}{2R}\left(\frac{\nu_B}{\nu_A}\right)^{1/2}\frac{\delta}{2} - \frac{v_o^1 - v_o^2}{2}(z-\delta)\right]t^{-1/2}, \qquad [30]$$

$$\lim_{t\to\infty} v_r^{B_2} = k\frac{R}{(\pi\nu_A)^{1/2}}\,\delta t^{1/2} + \frac{v_o^1 + v_o^2}{2} + u_o\frac{R}{(\pi\nu_A)^{1/2}}\frac{\delta}{2}t^{-1/2} - \frac{1}{(\pi\nu_B)}\left[\frac{(R^2+1)v_o^1 + (R^2-1)v_o^2}{2R}\left(\frac{\nu_B}{\nu_A}\right)^{1/2}\frac{\delta}{2} - \frac{v_o^1 - v_o^2}{2}z\right]t^{-1/2}. \qquad [31]$$

In all the long-time asymptotes there is a simple time dependence, dominated after intermediate or even early times by the pressure-driven flow in the film which sets the adjoining fluid into identical motion. Different initial velocity fields, for example, giving rise to momentum interchange between phases have an effect, but one which eventually dies out relative to the pressure contribution. It is at first surprising that the pressure force in the film is so effective in the adjoining phases, there being no attenuation whatsoever: the film eventually moves as a rigid body and so does the fluid on either side. Although the amount of B-phase fluid so set in motion must grow in time, it evidently reaches a stage beyond which growth is slow relative to the large mass of fluid already set into effectively rigid-body motion and consequently in which there is no further appreciable retardation of motion. The "ground-state" for long-time motion is not u_o, but the arithmetic mean of the initial motion in the B-phases. The motion in all three phases grows inexorably in time due to the momentum source k, but it does so at an ever decreasing rate.

Because the long-time asymptote v_r^A ($t \to \infty$) is only a slowly-varying function of time, it is natural to attempt a comparison with the steady solutions associated with the decoupling boundaries of earlier, simpler models. They provide for parabolic velocity profiles in the film if either or both interfaces are "rigid", and if both are "free" the model leads to an infinite velocity prediction. Moreover, decoupled models do not provide for motion in the contiguous phase(s) (or if there were, it would be independent of motion in the film). In contrast, coupled motions are of the essence in real systems *and* in the present model, two prominent features of which are the "velocity defects" between film and contiguous phases leading to momentum interchange and momentum increase in contiguous phases due to pressure-driven flow in the film. The latter become ever more effective with elapse of time, as mentioned above, and eventually move all three phases effectively as a single solid body. The former can be dominant early in drainage, and it can happen that initially the more rapid film flow can transport momentum to the other phases before pressure forces become significant; should drop or homophase circulation be initially greater, then film motion is correspondingly enhanced and coalescence consequently hastened. Provided that appreciable dimpling does not occur or that instability which can lead to film rupture (coalescence) does not occur, pressure forces ultimately dominate flow in all three phases, whereas they are quickly balanced by viscous forces for two rigid planes bounding the film—although the initial motions in the three phases can survive and influence motion in the film for intermediate times.

The case $R = 1.01$ was selected for calculations on physical grounds, for a system having equal dynamic viscosities is important as a basic system, yet there must be a density difference to effect drainage. Moreover, if R is identically unity, no series expansion is required to invert the ancillary expressions for the velocity fields, which are then

$$\tilde{u}_A = -\left(\frac{\tilde{k}+u_o}{2}\right)\frac{[e^{-q_A(\delta-z)}+e^{-q_A z}]}{s}+\frac{\tilde{k}+u_o}{s}+\frac{1}{2}\frac{[v_o^1 e^{-q_A(\delta-z)}+v_o^2 e^{-q_A z}]}{s}, \qquad [32]$$

$$\tilde{u}_{B_1} = \left(\frac{\tilde{k}+u_o}{2}\right)\frac{[e^{q_B(\delta-z)}-e^{q_B(\delta-z)-q_A\delta}]}{s}-\frac{1}{2}\frac{[v_o^1 e^{q_B(\delta-z)}-v_o^2 e^{q_B(\delta-z)-q_A\delta}]}{s}+\frac{v_o^1}{s}, \qquad [33]$$

$$\tilde{u}_{B_2} = \left(\frac{\tilde{k}+u_o}{2}\right)\frac{[e^{q_B z}-e^{q_B z-q_A\delta}]}{s}+\frac{1}{2}\frac{[v_o^1 e^{q_B z-q_A\delta}-v_o^2 e^{q_B z}]}{s}+\frac{v_o^2}{s}. \qquad [34]$$

The inverse transformations are then readily performed (Abramowitz & Stegun 1968) to give

$$v_r^A = kt\left\{1-2i^2\operatorname{erfc}\left(\frac{\delta-z}{(4\nu_A t)^{1/2}}\right)-2i^2\operatorname{erfc}\left(\frac{z}{(4\nu_A t)^{1/2}}\right)\right\}$$
$$+u_o+\left(\frac{v_o^1-u_o}{2}\right)\operatorname{erfc}\left(\frac{\delta-z}{(4\nu_A t)^{1/2}}\right)+\left(\frac{v_o^2-u_o}{2}\right)\operatorname{erfc}\left(\frac{z}{(4\nu_A t)^{1/2}}\right). \qquad [35]$$

$$v_r^{B_1} = kt\left\{2i^2\operatorname{erfc}\left(\frac{z-\delta}{(4\nu_B t)^{1/2}}\right)-2i^2\operatorname{erfc}\left(\frac{(z-\delta)+\left(\frac{\nu_B}{\nu_A}\right)^{1/2}\delta}{(4\nu_B t)^{1/2}}\right)\right\}$$
$$+\frac{u_o-v_o^1}{2}\operatorname{erfc}\left(\frac{z-\delta}{(4\nu_B t)^{1/2}}\right)+\frac{v_o^2-u_o}{2}\operatorname{erfc}\left(\frac{(z-\delta)+\left(\frac{\nu_B}{\nu_A}\right)^{1/2}\delta}{(4\nu_B t)^{1/2}}\right)+v_o^1, \qquad [36]$$

$$v_r^{B_2} = kt\left\{2i^2\operatorname{erfc}\left(\frac{-z}{(4\nu_B t)^{1/2}}\right)-2i^2\operatorname{erfc}\left(\frac{\left(\frac{\nu_B}{\nu_A}\right)^{1/2}\delta-z}{(4\nu_B t)^{1/2}}\right)\right\}$$

$$+\frac{v_o^1 - u_o}{2}\operatorname{erfc}\left(\frac{\left(\frac{v_B}{v_A}\right)^{1/2}\delta - z}{(4v_B t)^{1/2}}\right) + \frac{u_o - v_o^2}{2}\operatorname{erfc}\left(\frac{-z}{(4v_B t)^{1/2}}\right) + v_o^2. \quad [37]$$

In this simple but practically significant special case, motion is dominated for long times by the pressure-driven film drainage. Appropriate asymptotic formulae for small arguments (Abramowitz & Stegun 1968) can be used to get the long-time asymptotes, for neither here nor in the general formulae can one obtain the correct answer by simply setting $t = \infty$:

$$\lim_{t\to\infty} v_r^A = \frac{k\delta}{(\pi v_A)^{1/2}}t^{1/2} + \frac{u_o\delta}{2(\pi v_A)^{1/2}}t^{-1/2} + \frac{v_o^1 + v_o^2}{2} - \frac{v_o^1(\delta - z) + v_o^2 z}{2(\pi v_A)^{1/2}}t^{-1/2}, \quad [38]$$

$$\lim_{t\to\infty} v_r^{B_1} = \frac{k\delta}{(\pi v_A)^{1/2}}t^{1/2} + \frac{u_o\delta}{2(\pi v_A)^{1/2}}t^{-1/2} + \frac{v_o^1 + v_o^2}{2} + \frac{1}{2(\pi v_B)^{1/2}}\left[(v_o^1 - v_o^2)(z - \delta) - v_o^2\left(\frac{v_B}{v_A}\right)^{1/2}\delta\right]t^{-1/2}, \quad [39]$$

$$\lim_{t\to\infty} v_r^B = \frac{k\delta}{(\pi v_A)^{1/2}}t^{1/2} + \frac{u_o\delta}{2(\pi v_A)^{1/2}}t^{-1/2} + \frac{v_o^1 + v_o^2}{2} + \frac{1}{2(\pi v_B)^{1/2}}\left[(v_o^1 - v_o^2)z - v_o^1\left(\frac{v_B}{v_A}\right)^{1/2}\delta\right]t^{-1/2}. \quad [40]$$

As expected intuitively, the initial conditions play a prominent role for short times. Analogous calculations, this time using formulae corresponding to large arguments, yield

$$\lim_{t\to 0} v_r^A = kt\left\{1 - \frac{4}{\pi^{1/2}}(v_A t)^{3/2}\left[\frac{1}{z^3}\exp\left(-\frac{z^2}{4v_A t}\right) + \frac{1}{(\delta - z)^3}\times\exp\left(-\frac{(\delta - z)^2}{4v_A t}\right)\right]\right\} + \frac{1}{\pi^{1/2}}(v_o^1 - u_o)(v_A t)^{1/2}\left(\frac{1}{\delta - z}\right)\exp\left(-\frac{(\delta - z)^2}{4v_A t}\right) + \frac{1}{\pi^{1/2}}(v_o^2 - u_o)(v_A t)^{1/2}\left(\frac{1}{z}\right)\exp\left(-\frac{z^2}{4v_A t}\right) + u_o, \quad [41]$$

$$\lim_{t\to 0} v_r^{B_1} = \frac{4kt}{\pi^{1/2}}(v_B t)^{3/2}\left\{\frac{1}{(z - \delta)^3}\exp\left(-\frac{(z - \delta)^2}{4v_B t}\right) - \frac{1}{\left[(z - \delta) + \left(\frac{v_B}{v_A}\right)^{1/2}\delta\right]^3}\times\exp\left(-\frac{\left(z - \delta + \left(\frac{v_B}{v_A}\right)^{1/2}\delta\right)^2}{4v_B t}\right)\right\} + \frac{1}{\pi^{1/2}}(u_o - v_o^1)\frac{(v_B t)^{1/2}}{z - \delta}\exp\left(-\frac{(z - \delta)^2}{4v_B t}\right) + v_o^1 + \frac{1}{\pi^{1/2}}(v_o^2 - u_o)\frac{(v_B t)^{1/2}}{(z - \delta) + \left(\frac{v_B}{v_A}\right)^{1/2}\delta}\exp\left(-\frac{\left(z - \delta + \left(\frac{v_B}{v_A}\right)^{1/2}\delta\right)^2}{4v_B t}\right), \quad [42]$$

$$\lim_{t\to 0} v_r^{B_2} = \frac{4kt}{\pi^{1/2}}(\nu_B t)^{3/2}\left\{\frac{1}{(-z)^3}\exp\left(\frac{-z^2}{4\nu_B t}\right) - \frac{1}{\left[\left(\frac{\nu_B}{\nu_A}\right)^{1/2}\delta - z\right]^3} \times \exp\left(-\frac{\left(\left(\frac{\nu_B}{\nu_A}\right)^{1/2}\delta - z\right)^2}{4\nu_B t}\right)\right.$$

$$+ \frac{v_o^1 - u_o}{\pi^{1/2}}\frac{(\nu_B t)^{1/2}}{\left(\frac{\nu_B}{\nu_A}\right)^{1/2}\delta - z}\exp\left(-\frac{\left(\left(\frac{\nu_B}{\nu_A}\right)^{1/2}\delta - z\right)^2}{4\nu_B t}\right)$$

$$- \frac{u_o - v_o^2}{\pi^{1/2}}\frac{(\nu_B t)^{1/2}}{z}\exp\left(-\frac{z^2}{4\nu_B t}\right) + v_o^2. \qquad [43]$$

4. DISCUSSION OF RESULTS

The exact solutions being difficult to interpret and the asymptotic forms being necessarily approximate, some summations of the series solutions are discussed in this section. The instantaneous vertical dependence of a typical, radially outward flow in the film and adjacent phases is depicted schematically in figure 1. Because of axial symmetry, subsequent figures show the evaluation of profiles in a single axial plane, with the reader cautioned that the independent variable ζ has been measured in units of δ within the film but in units of $\delta(\nu_B/\nu_A)^{1/2}$ outside the film in order to avoid introduction of an additional parameter.

Also by way of prefatory remarks, we note that the kinematic viscosity enters the equations of motion whereas the dynamic viscosity enters the boundary conditions. For the rectilinear motion considered here, the physical parameters appearing in the solutions for

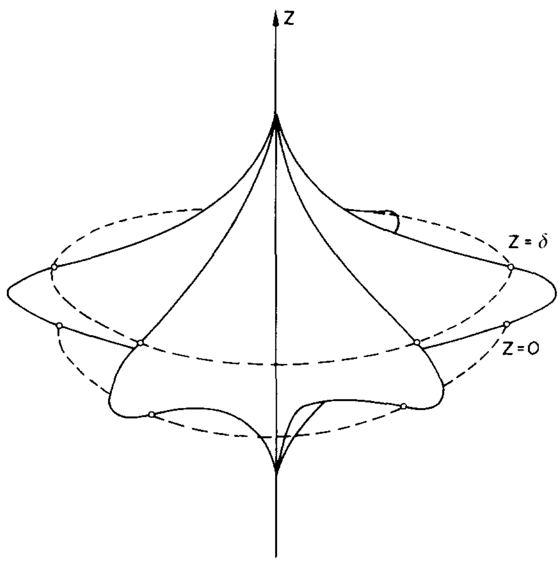

Figure 1. Schematic representation of an instantaneous velocity profile.

the velocity fields are consequently v_A, v_B and $R = (\mu_A \rho_A / \mu_B \rho_B)^{1/2}$. If the fluids are of comparable density, then $R \approx (\mu_A/\mu_B)^{1/2}$. Hence, in the sequel we shall speak of films being more viscous than their contiguous phases—or simply, more viscous—when the more precise but physically less suggestive statement that $R > 1$ applies; similar remarks hold for the cases $R \approx 1$, $R < 1$. This lack of precision is not without its pitfalls, but it has the clear advantage of intuitive appeal.

The range of values of R for real systems is extremely wide. The values $R = 10, 0.1$ are reciprocals, they represent a range of two full orders of magnitude, and they are adjudged reasonable bounds to demonstrate the effect of small and large R. The value 1.01 was selected as representing a system of equal viscosities yet having the requisite, but only slightly different, densities. For want of space, however, not all the results that are discussed have been presented, but a number of interesting situations for short-time behavior and interactions of several fields are explicitly explored.

Development of velocity profiles during later stages of drainage

It was demonstrated analytically that in the long-time limit film motion due to the pressure gradient eventually dominates initial flow fields in all phases and sets large—and ever larger—quantities of fluid on each side of the film into motion. An estimate of the time required to achieve the asymptotic flow conditions, as well as a feel for the approach to the asymptote, can be gotten from figures 2–4, where uniform initial conditions have been supposed and velocity profiles measured from the initial one are plotted against time for several values of R (viz., films much more, much less, and comparably viscous). The corresponding asymptotic results are shown as dashed curves. If the fluids are of comparable viscosity, as well as density (figure 2), the profiles evolve in a not unexpected manner; in particular, for short times film flow appears almost parabolic, although that tendency is

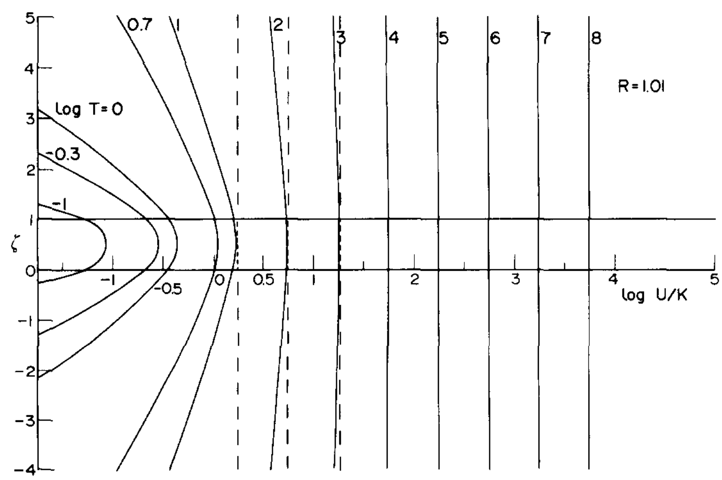

Figure 2.

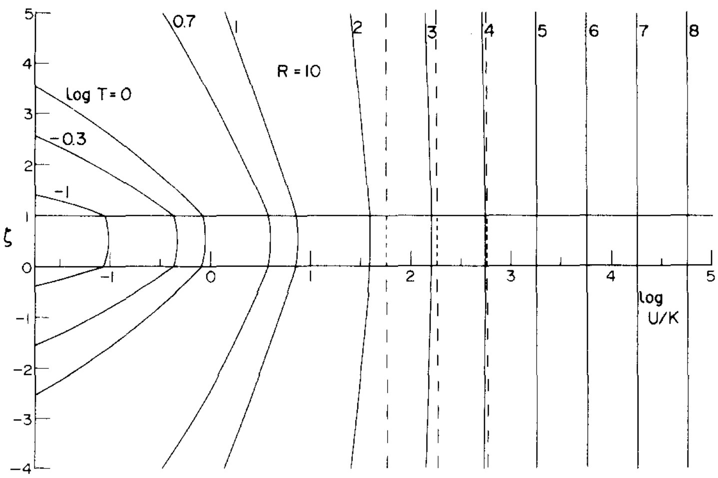

Figure 3.

immediately and continuously offset by momentum transported across the interfaces. The more viscous the film is relative to the other phase (figure 3), the more it tends to move as a rigid body from the outset, inasmuch as the contiguous phases are more easily set in motion. For the converse case of a less viscous film (figure 4), the film is more readily set into motion,

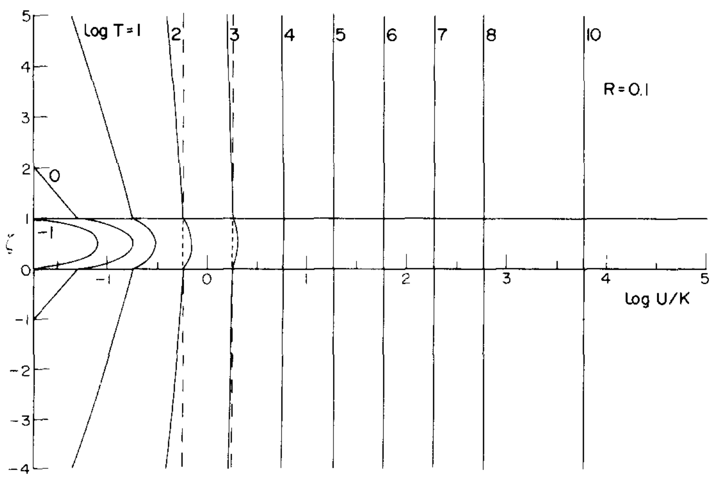

Figure 4.

Figures 2–4 (taken together). Effect of physical properties on the development of velocity profiles measured from a uniform initial velocity. $U = (v_r - v_r^o)\delta/\nu_A$; $K = k\delta^3/\nu_A^2$; $T = \delta^2/\nu_A$.

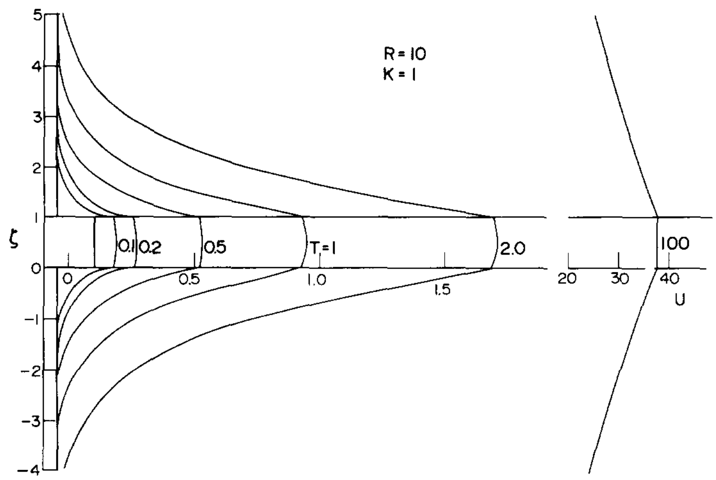

Figure 5.

and in fact the shorter the time and the more viscous the contiguous phases, the more parabolic is the velocity profile in the film.

In addition to the above purposes, figures 2–4 can be used to interpret systems having initially non-uniform motion after intermediate times when most of these initial transients have died out (cf. especially figures 5–9).

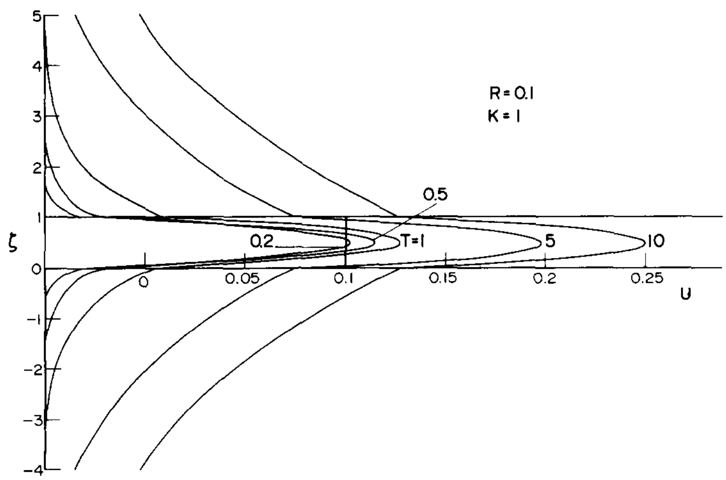

Figure 6.

Figures 5 and 6. Effect of physical properties on the development of velocity profiles for non-uniform initial velocities. $U = v_r\delta/\nu_A$; $K = k\delta^3/\nu_A^2$; $T = \delta^2/\nu_A$; $U_o^A = 0.1$; $U_o^B = -0.05$.

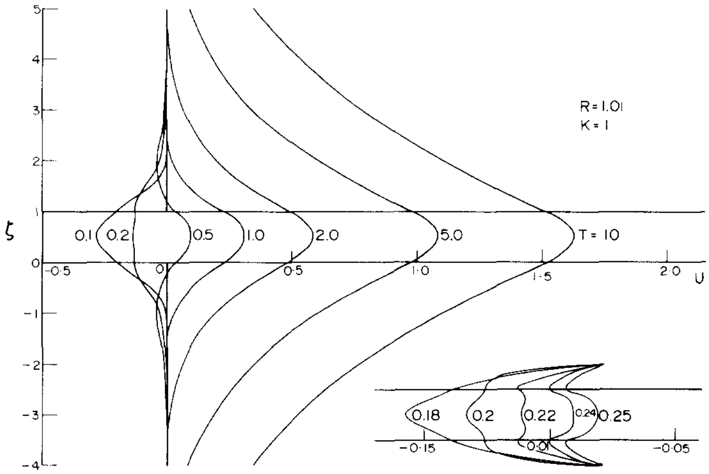

Figure 7. Reversal of inward film drainage. $U_o^A = -0.5$; $U_o^B = 0$.

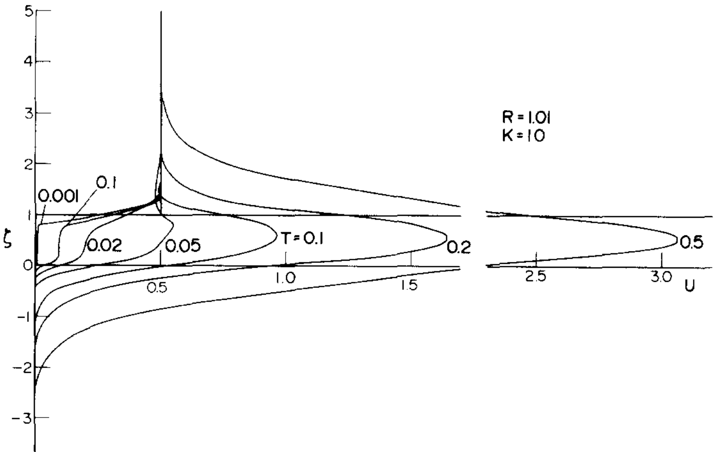

Figure 8.

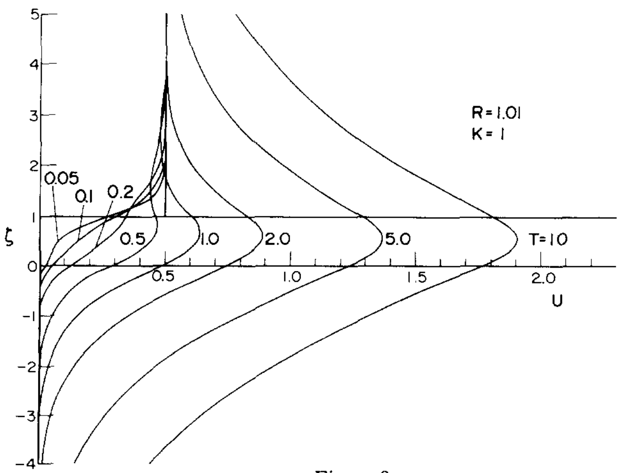

Figure 9.

Drainage in systems having films less viscous than adjacent phases

For an initially quiescent system the pressure gradient enters the velocity expressions for all three regions [23]–[25] as a constant, multiplicative factor, as indeed it does if initial motion is only uniform. If the film is much less viscous than the drop and its homophase, the velocity profile within the film has a somewhat parabolic appearance at any instant of time, an effect the more pronounced the shorter the time (figure 4). Unfortunately for even this tenuous comparison with static profiles in films decoupled from their surroundings by unrealistic boundary conditions, however, the film velocity neither remains constant nor does it vanish at the bounding surfaces.

For moderately asymmetric initial conditions, an instantaneously parabolically shaped film profile can occur for intermediate times long enough that the asymmetry has been overcome but short enough that the contiguous phases have not yet begun to overtake the film motion. A reduction of the pressure gradient by an order of magnitude permits more interaction of the initial profiles due to diffusion, and the initial conditions dominate until longer times.

If the initial motion in the drop and its homophase is the same, regardless of that in the film, a symmetric profile necessarily occurs, at least in the absence of hydrodynamic instabilities. For the less viscous film initially flowing outward but counteracted by motion in the other two regions that is oppositely directed and an order of magnitude smaller, a dimensionless pressure gradient of order unity is at first barely able to maintain outflow. A thin disk of outflow eventually thickens and expands due to pressure forces, but only after it had perceptibly thinned because momentum diffused more quickly from the film than it could be restored by the pressure-gradient source.

The implication for coalescence hydrodynamics, in agreement with intuition and experimental observations (Hartland 1970, 1960) is that reverse flow in the drop could initially lead to thickening of the film. In addition to the quantification of a plausible notion, one sees a larger quantitative proposition, namely, that large disparities between outward film motion and drop and homophase motion can cause dramatic deceleration of film motion and, if the latter were inward, even reversal of film flow. The larger the pressure gradient, the less momentum diffuses from the film before it and its surroundings have been set in motion. The weight of the drop effects film flow through the pressure gradient set up in the film, and this of course subsequently overcomes the thickening tendency.

If the film flow inward is due to an abnormal pressure gradient and both are ultimately reversed by gravitational forces, such cases may be modelled by presuming null flow initially in drop and homophase with negative flow initially in the film. The flow reversal and accomplishment of normal drainage is inevitably associated with serpentine profiles (shown for $R = 1.01$ in figure 7), with momentum diffusion for short times dominating pressure effects and with pressure forces dominating the central portion of the film more easily than the layers near the interface, a combination of effects the more pronounced within the film the smaller is R. The asymptotic approach of $R \to 0$ recovers results reported elsewhere (Riolo, Reed & Hartland 1973).

Drainage in systems having films more viscous than adjacent phases

If the film is much more viscous than its neighboring phases, its velocity profile tends to be flatter, its motion tends to be dominant, and steeper velocity profiles occur in the adjacent phases. Thus, because it is more viscous it moves more like a solid, and small velocity gradients can nevertheless transmit momentum to the surroundings at a significant rate. Too, the surroundings are more easily sheared (figures 3 and 5).

The reversal of inward film flow in a more viscous film also manifests serpentine profiles but with their distortions, or curvature, less within the film, greater outside. The developing oscillatory boundary layer for larger R is a more pronounced analog of that on an oscillating flat plate just set into motion than that for smaller R because the film is more viscous relative to surroundings. A reduction in pressure permits greater instantaneous equilibration of film and surroundings. The interaction of pressure forces with nonuniform initial conditions more generally is such that a reduction in the pressure gradient permits more momentum to diffuse to or from the surroundings before the film further accelerates outward, an observation having wider validity.

Drainage in systems having films and adjacent phases of comparable viscosities

The range $0.1 \leq R \leq 10$ scarcely brackets the variety of physical systems occurring in industrial practice and fundamental research, nor do the cases considered above exhaust the situations and phenomena occurring in drainage hydrodynamics for even these systems. It is therefore all the more desirable to select a base system and attempt a more complete compilation. The base system that suggests itself directly is that of comparable viscosities, and the base case would be an initially quiescent system subjected to a dimensionless pressure gradient of unity, shown as the special case $K = 1$ in figure 2. As symmetric, and therefore uniform, initial conditions are mapped by the differential equations into symmetric solutions (independently of R) when both adjacent phases begin with the same motion (figure 7), the behavior soon looks like that for uniform initial motion (figure 2), regardless of the magnitude and sign of the initial difference in u_o and $v_o^1 = v_o^2$. It is only a matter of initial transients being different and taking longer to die out the smaller the pressure gradient is and the larger the initial velocity difference is. The quantitative features of the early transients are certainly distinct, but there is nothing to qualitatively distinguish them, with the exception that for asymptotically small and vanishing pressure gradients the diffusion limit is recovered (see figures 8–11).

If the initial conditions are asymmetric with the drop initially moving faster than the film (figures 8–11), the drop profiles manifest oscillatory boundary layer development, and the film profiles have pronounced points of inflection, except in the limit of vanishing pressure gradients, where the initial value problem for pure diffusion is recovered (figure 11). The weaker the pressure forces, the more momentum is interchanged by diffusion between drop and film—and hence between film and homophase—before pressure begins to effect drainage (cf. figures 9 and 10) and the better the drop and homophase motions are able to equilibrate to the pressure-driven film motion. For greater pressure forces, there is less momentum interchanged before drainage occurs, and certainly none *across* the film to the

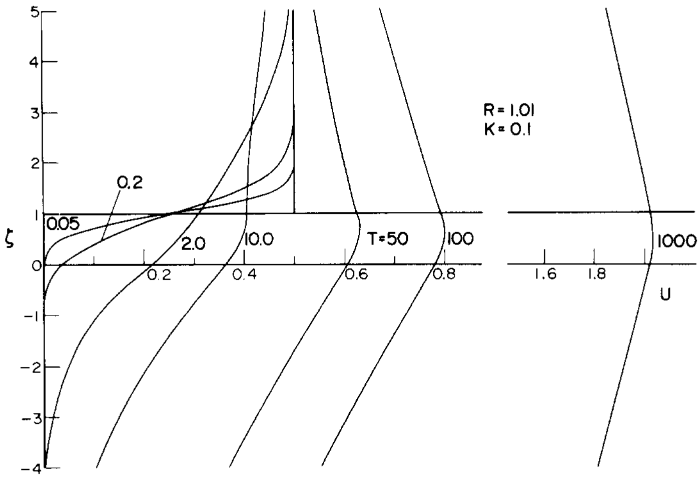

Figure 10.

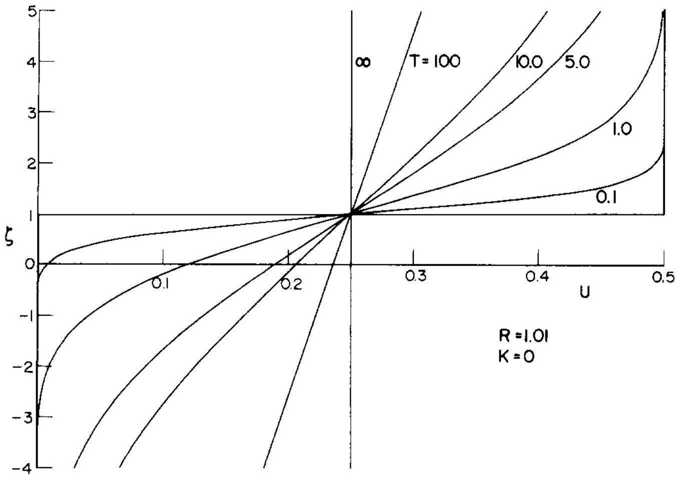

Figure 11.

Figures 8–11. Effect of pressure on the development of velocity profiles for outward drop circulation initially. $U_o^A = U_o^{B_2} = 0$; $U_o^{B_1} = 0.5$.

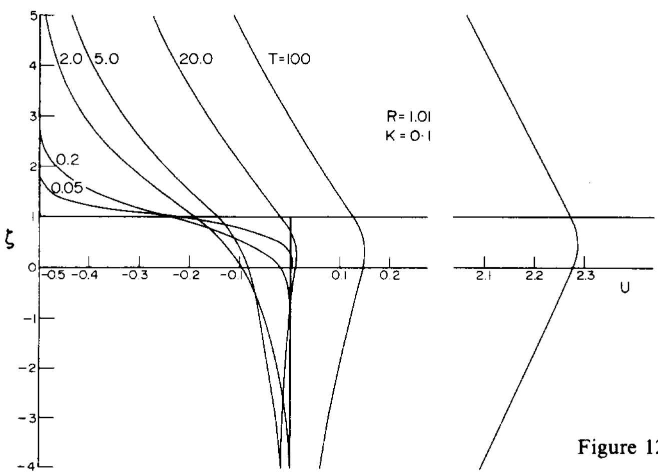

Figure 12. $U_o^{B_1} = -0.5$.

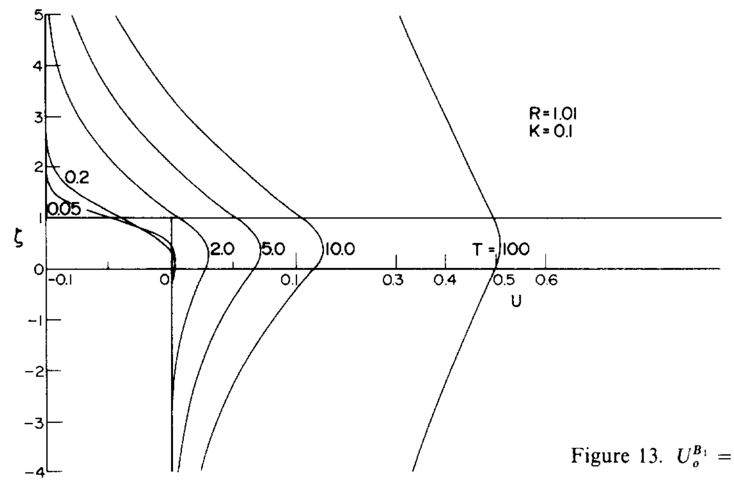

Figure 13. $U_o^{B_1} = -0.1$.

Figures 12 and 13. Effect of initially inwards circulation in the drop on the development of velocity profiles. $U_o^A = U_o^{B_2} = 0$.

homophase (cf. figures 8 and 9). Except for very short times, the profiles generated when there is no initial film motion differ little from those when there is film motion, provided the drop motion is greater.

The preceding cases were important for the practical reason that they quantify intuition concerning the role that normal circulation within the drop plays in enhancing drainage of the film. Reverse circulation has an equally significant effect, for then the pressure gradient must act to overcome inward motion in the film set up by the initial (negative) velocity difference. This effect is heightened with decreased pressure gradients, as would be expected, although any tendency toward thickening of the film due to influx of the fluid is finally overcome by pressure forces with further elapse of time. The pattern of motion is shown in figures 12 and 13 for different rates of reverse drop circulation.

If the initial reverse motion is in the film and there is comparable but oppositely directed initial motion in the drop, asymmetric profiles result, in which familiar transients for short times appear and for which the diffusive contribution outweighs pressure forces the weaker the latter become. Ultimately—except for truly miniscule pressure effects—the profiles take on forms in which initial conditions are virtually erased. In the limit of miniscule pressure gradients, pure diffusion profiles are recovered.

Reverse drop circulation having brought about inward flow in the film, it is of practical interest to know how the pressure gradient reverses the motion and brings about drainage. A result in this direction is shown for plausible initial conditions in figure 7. The profiles within the film and in the adjacent phases have already been mentioned, but the hydrodynamic interaction of the phases across their common interfaces during the period of flow reversal is of fluid mechanical interest, as well as practical importance. The flow in the drop bears a strong resemblance to that in the boundary layer developing on a flat plate that has just been set into oscillatory motion parallel to itself. The inwardly directed film flow initiates reverse circulation in the drop at the expense of inward flow at the boundary regions of the film. The flatter profile in the interior of the film offers less viscous resistance to tendencies of outward flow in response to the pressure gradient. The interior of the film can thus overtake the exterior of the film, with resultant serpentine profiles in the film (emphasized by the enlarged velocity scale and reduced vertical scale selected in the insert to figure 7 but also visible on the original scale). At the same time that a reverse circulation is penetrating into the interior of the drop and its homophase from the initially inward film flow, the newly initiated film outflow reverses that tendency in the immediate neighborhood of the interfaces. The resulting profiles outside the film have the appearance of boundary layers developing during the initial period of oscillation of a flat plate parallel to itself, a recurrent theme in all cases of film flow reversal. Similarly, inflection points and more general serpentine profiles within the film recur under other similar circumstances of flow reversal.

5. CONCLUSIONS

The drainage of thin films that are hydrodynamically coupled with their adjacent phases differs completely from drainage between immobile boundaries. The flow depends upon the pressure gradient driving the film flow—and hence also flow in contiguous phases—and upon the initial conditions in all three phases. The flow in the three phases also depends strongly upon their physical properties in the form of $(\nu_B/\nu_A)^{1/2}$, the kinematic viscosity ratio, and $R = (\rho_A\mu_A/\rho_B\mu_B)^{1/2} = (\mu_A/\mu_B)(\nu_B/\nu_A)^{1/2}$, a dimensionless parameter characterizing the ratios of two kinds of momentum transport in the two phases, on the one hand at the boundary between the two phases, and on the other in the interiors of the two phases.

Several properties can be inferred from the exact solution, ranging from symmetry conditions to physical interpretations of individual terms (Section 2). Other analytical information can be extracted from asymptotic forms of the solutions (Section 3). In particular, for short to intermediate times the flow disparities in the three regions determine the flow profiles, but for longer times the pressure gradient completely dominates flow in all three phases. A steady asymptotic form is not attained, regardless of the time.

The role of physical properties is more pronounced, the shorter the time; the meaning of R and its effect on the velocity profiles can hence best be seen for short times. A proper yet simple comparison of different systems that also elucidates R is as follows. Consider a given film having distinct surroundings in the two cases, yet with kinematic viscosities the same in both phases in both cases and with pressure forces and initial velocity differences the same in both cases. If R is small, the film may be described as less viscous than its surroundings. It is therefore more easily set into motion, whereas its surroundings remain relatively quiescent until the steepening velocity profiles within the film begin transferring more momentum to them. Conversely, if R is large, the film is the more viscous, the surroundings more easily sheared, and the film sets off almost as a rigid body. For comparably viscous systems, however, the surroundings begin to receive momentum almost immediately because they offer immediate resistance that leads to early velocity gradients within the film. Moreover, the smaller the pressure gradient and the larger the initial flow disparities, the more is diffusional interaction responsible for the development of velocity profiles during the early stages of drainage, with R modulating the dimensionless profiles.

The foregoing conclusions based on analytical but asymptotic arguments are reinforced and quantified by summation of the series solutions (Section 4). Quite unusual velocity profiles can occur due to drop circulation or reverse film flow, for instance, for the physical complexity of drainage in three-phase systems is faithfully mirrored to that extent in the mathematical complexity of the analytical solutions. The numerically generated profiles can also help to extend and refine intuition developed from the asymptotic formulae and presented as conclusions above, provided proper computational care is exercised.

The convergence criterion for the subroutine calculation of each mathematical function in the series can cause problems with the convergence, or more accurately, with the accuracy, of the summation of the series itself, although there is no fundamental difficulty. Certain situations are, however, awkward in principle as well as in calculation. For example, for short times the $R \rightarrow 0$ limit may be computed directly from the formulae, but for longer times computation becomes increasingly difficult until, at $R = 0$, round-off errors cause failure unless the series is first manipulated into another form (cf. Riolo, Reed & Hartland 1973). The physical basis of this difficulty is readily understood, for there is very little penetration of motion into the adjacent phases for sufficiently small R and short times, even for large pressure gradients; but so long as R is not identically zero there must eventually be motion in the surroundings in consequence of that in the film.

In a companion paper the implications for film-thinning of such microflow situations as have been described here will be analyzed.

Acknowledgement—We would like to thank the "Schweizerischen Nationalfonds zur Förderung der wissenschaftlichen Forschung" and the "Schweizerischen chemischen Industrie" for financial assistance.

REFERENCES

Abramowitz, M. & Stegun, I. A. 1968 *Handbook of Mathematical Functions*. Dover.

Allan, R. S. & Mason, S. G. 1962 Particle motions in sheared suspensions, XIV. *J. Colloid Sci.* **17**, 383–408.

Carslaw, H. S. & Jaeger, J. C. 1959 *Heat Conduction in Solids*. Oxford University Press.

Hartland, S. 1967 The approach of a liquid drop to a flat plate. *Chem. Engng Sci.* **22**, 1675–1687.

Hartland, S. 1969 The shape of a fluid drop approaching an interface. *Can. J. Chem. Engng* **47**, 221–225.

Hartland, S. 1969 The profile of the draining film beneath a liquid drop approaching a plane interface. *Chem. Engng Prog. Symposium Series* **65**, 82–89.

Hartland, S. 1969 The profile of the draining film between a rigid sphere and a deformable fluid–liquid interface. *Chem. Engng Sci.* **24**, 987–995.

Hartland, S. 1969 The effect of circulation patterns on the drainage of the flow between a liquid drop and a deformable liquid–liquid interface. *Chem. Engng Sci.* **24**, 611–613.

Hartland, S. 1970 *The Coalescence of Liquid Drops.* British Universities Film Council.

Hartland, S. 1971 The pressure distribution in axisymmetric draining films. *J. Colloid Int. Sci.* **35**, 227–237.

Hartland, S. 1972 The effect of surface active agents on the coalescence of liquid drops. *Proc. VI. Int. Cong. Surface Activity.* Zürich.

Hartland, S. & Wood, S. 1973 Effect of applied force on the approach of a drop to a fluid–liquid interface. *A.I.Ch.E.J.* **19**, 871–876.

McKay, G. D. M. & Mason, S. G. 1964 Particle motions in sheared suspensions, XV. *Kolloid Z.* **195**, 138–148.

Murdoch, P. G. & Leng, D. E. 1971 The mathematical formulation of hydrodynamic film thinning and its application to colliding drops suspended in a second liquid. *Chem. Engng Sci.* **26**, 1881–1892.

Princen, H. M. 1963 Shape of a fluid drop at a liquid–liquid interface. *J. Coll. Sci.* **18**, 178–195.

Reynolds, O. 1886 On the theory of lubrication. *Phil. Trans. R. Soc. Lond.* **A177**. 157–234.

Riolo, E., Reed, X. B. & Hartland, S. 1973 On initial transients in Reynolds' drainage model. *Chem. Engng J.* **6**, 121–128.

Robinson, J. D. & Hartland, S. 1971 Effect of adjacent drops on the shape of a drop approaching a deformable liquid–liquid interface. *Proc. Int. Solvent Extraction Conf.*, Vol. 1, pp. 418–427. The Hague.

Robinson, J. D. & Hartland, S. 1972 The effect of surface active agents on coalescence. *Tenside* **9**, 301–308.

Scheele, G. F. & Leng, D. E. 1971 An experimental study of factors which promote coalescence of two colliding drops suspended in water. *Chem. Engng Sci.* **26**, 1867–1879.

Wood, S. M. & Hartland, S. 1972 The shape of a drop trapped between two horizontal surfaces. *A.I.Ch.E.J.* **18**, 1041–1047.

Sommaire—L'effet d'accouplement hydrodynamique de phases adjacentes sur le drainage de pellicules minces est examiné à l'aide d'un modèle prototype de coalescence. Pur de longues périodes les forces de pression dans la pellicule dominent l'écoulement dans les trois régions, et finalement elles se meuvent toutes effectivement comme une seule tandis que pour les courtes périodes, les profils sont aigüs et les différences initiales d'écoulement dans les trois régions peuvent dominer les effets de pression. Pour les durées intermédiaires, l'évolution temporelle des profils de vélocité dépend de façon compliquée du rapport de viscosité cinématique et du paramètre $R = (\rho_A \mu_A/\rho_B \mu_B)^{1/2}$, ainsi que des conditions initiales et du gradient de pression. De façon générale, les écoulements initiaux ont moins d'effet sur le temps total de drainage que la présence de circulation induite dans les phases adjacentes. Des solutions analytiques sont relevées pour une gamme de systèmes, des conditions initiales représentatives, et des gradients de pression. Dans un article suivant, des équations d'amincissement de pellicule sont résolues à l'aide de ces renseignements.

Auszug—Es wird die Wirkung hydrodynamischer Kopplung von anliegenden Phasen auf die achsensymmetrische Abfliessen des Filmes dünner Filme mittels eines Prototyps eines Koaleszenzmodells untersucht. Für lange Zeit beherrschen Druckkräfte in dem Film den Fluß in allen drei Bereichen und dann gehen alle praktisch in einen einzelnen über, während für kurze Zeit Profile scharf ausgeprägt sind, und anfängliche Strömungsunterschiede in den drei Bereichen können Druckwirkungen beherrschen. Für Zwischenzeiten hängt die zeitliche Evolution der Geschwindigkeitsprofile in einer komplizierten Weise von dem Verhältnis der kinematischen Viskosität und dem

Parameter $R = (\rho_A\mu_A/\rho_B\mu_B)^{1/2}$ sowie von den anfänglichen Bedingungen und dem Druckgefälle ab. Im allgemeinen haben die anfänglichen Flüsse eine geringere Wirkung auf gesamte Abflusszeit als das Vorhandensein von induzierter Zirkulation in anliegenden Phasen. Es werden analytische Lösungen für einen Bereich von Systemen und kennzeichnende Anfangsbedingungen und Druckgefälle diagrammatisch dargestellt. In einem darauffolgenden Bericht werden Filmabnahmegleichungen auf Grund dieser Information gelöst.

Резюме—При помощи прототипа модели коалесценции исследуют эффект гидродинамического взаимодействия соседних фаз на осесимметричное свободное стекание тонких пленок. В длительные периоды времени, сила давления в пленке доминирует над потоком во всех трех областях, но в конце концов все эффективно перемещаются как единое целое, в то время как в короткие промежутки времени профили резкие и разности исходного течения во всех областях могут повлиять на давление. В промежуточное время, переходящее развитие профилей скорости зависит от сложных фактов—от степени кинематической вязкости и параметра $R = (\rho_A\mu_A/\rho_B\mu_B)^{1/2}$, также как и от исходных условий и градиента давления. Как правило, исходные потоки меньше влияют на время общего свободного стекания, чем присутствие индуцированной циркуляции в соседней фазе. Планируют аналитические решения для ряда систем, показательные исходные условия и градиенты давления. В следующей статье решают уравнения разжижения пленки при помощи этой информации.